

Efficient wireless charging of a quantum battery

Ming-Liang Hu,^{1,*} Ting Gao,¹ and Heng Fan^{2,3,4,†}

¹*School of Science, Xi'an University of Posts and Telecommunications, Xi'an 710121, China*

²*Institute of Physics, Chinese Academy of Sciences, Beijing 100190, China*

³*School of Physical Sciences, University of Chinese Academy of Sciences, Beijing 100190, China*

⁴*Beijing Academy of Quantum Information Sciences, Beijing 100193, China*

We explore the wireless charging of a quantum battery (QB) via n charging units, whose coupling is mediated by a common bosonic reservoir. We consider the general scenarios in which the charger energy is not maximal and the QB has residual ergotropy initially. It is found that the charging performance improves with the increase of the coupling strength. In the strong coupling regime, the charging time is insensitive to the charger energy, the number of charging units, and the residual ergotropy in the QB, while the ergotropy charged on the QB strongly depends on the charger energy and ergotropy, and the residual ergotropy in the QB does not help to enhance its performance. Moreover, the multiple charging units help to enhance the charging performance in the weak and moderate coupling regimes, while they are less efficient in the strong coupling regime.

I. INTRODUCTION

Quantum battery (QB) is a microscopic quantum mechanical device used to temporarily store and release energy in a controllable manner. The idealized procedure of work extraction from a QB is implemented via a cyclic unitary transformation of it governed by the system dynamics plus some controlling fields in a certain time interval. The maximal amount of extractable work in this process is termed as ergotropy [1], which is defined as the surplus energy of the initial state ρ of the QB with respect to the full set of passive states having the same eigenvalues as ρ . Here, a state σ is called passive if no work can be extracted from it by using any such unitary transformation [2–4], while it is called active if the maximal work output is nonzero. Moreover, the product of two independent copies of a passive state σ may not always be passive (σ is called completely passive if $\sigma^{\otimes n}$ is passive with respect to the sum Hamiltonian $H = \sum_{i=1}^n H_i, \forall n$), so the ergotropy for n collective QB cells may be different from the sum of ergotropies for n copies of a single-cell QB [1, 5].

Up to date, the QB was extensively studied from two main aspects. The first one, centering around the interplay between the performance of a QB and the various quantum resources, revealed that some of its figures of merit (ergotropy, charging power, battery capacity, etc.) are intimately related to quantum characteristics of the battery state such as entropy, coherence, and entanglement [6–19]. The second one, on the other hand, focused on the charging process of a QB, e.g., the possible realizations of a QB in the spin-chain systems [14, 20–23], the Tavis-Cummings model [9, 24], the harmonic oscillators [25–27], the Dicke model [28–31], and the three-level systems [27, 32]. For these battery models, numerous efforts have also been invested into devising feasible schemes to enhance their charging power [33–41], exploring their quantum advantages in the charging efficiency (time of charging, input power, total stored energy, etc.) [42–49], and identifying bounds on their extractable work and charging power [10, 50, 51]. Moreover,

as any quantum system is inevitably disturbed by its surrounding environment, and the charger and QB cannot be excluded from this process too, the dissipative charging of a QB has also been widely explored [12, 25, 52–66]; in particular, some structured reservoirs can be exploited as mediators for transferring energy from the charger to a QB, that is, to realize the wireless charging process [53, 54, 65].

Concerning the charging of a QB, our goal is to realize the fast charging and high charging capacity, and it is appealing to provide a general study on the details of the charging process under various situations. However, while most of the previous works considered the case that the charger energy is maximal and the QB is fully discharged initially, the charger might not always be in its fully excited state and one rarely waits until a battery runs out before charging in realistic situations. In fact, by considering different initial states of a QB driven by a classical force, it was found that an optimal charging is achieved if it starts from the ground state [67]. Inspired by this, we consider in this paper the general scenarios in which the charger energy is not maximal and the QB is not fully discharged initially, putting emphasis on the role of the number n of charging units and the amount of energy in the charger, the residual ergotropy in the QB, and the coupling strength of the system (i.e., charger + QB) to a common structured reservoir in controlling the charging time and the ergotropy. We will show that the charging performance mediated by the common reservoir improves with the increasing coupling strength, and intuitively, the multiple charging units and the residual ergotropy in the QB may not always be beneficial for shortening the charging time and enhancing the charged ergotropy.

The rest of the paper is organized as follows. In Sec. II, we recall the concept of ergotropy, then in Sec. III, we present the charger-battery model we considered. Sec. IV is devoted to analyzing the charging of a QB via n ($n \geq 1$) charging units. Finally, we summarize our findings in Sec. V.

II. PRELIMINARIES

In this section, we recall the notion of ergotropy and the related quantities. The ergotropy quantifies the maximal amount

*Electronic address: mingliang0301@163.com

†Electronic address: hfan@iphy.ac.cn

of work that can be reversibly extracted from a system (i.e., a QB). For a given QB with the free Hamiltonian H , the average work extractable from it by using a cyclic unitary transformation U is $\mathcal{W}(\rho, U) = \text{tr}(\rho H) - \text{tr}(U\rho U^\dagger H)$, and the ergotropy \mathcal{E} is defined as the maximum of \mathcal{W} , i.e.,

$$\mathcal{E} = \max_{U \in \mathcal{U}_c} \mathcal{W}(\rho, U), \quad (1)$$

where ρ is the battery state and the maximization is taken over the set of cyclic unitary operations \mathcal{U}_c in the Hilbert space \mathcal{H}_d ($d = \dim \rho$), and \mathcal{U}_c can be generated in a given time interval $[0, \tau]$ by applying suitable control fields to the system.

The optimal state $\tilde{\rho} = \tilde{U}\rho\tilde{U}^\dagger$, realizing the maximum in Eq. (1), is called the passive state associated with ρ . By rewriting ρ in its eigenbasis as $\rho = \sum_j r_j |r_j\rangle\langle r_j|$ and H in its eigenbasis as $H = \sum_k \varepsilon_k |\varepsilon_k\rangle\langle \varepsilon_k|$, where their respective eigenvalues are reordered as $r_j \geq r_{j+1}$ ($\forall j$) and $\varepsilon_k \leq \varepsilon_{k+1}$ ($\forall k$), the optimal unitary can be obtained as $\tilde{U} = \sum_j |\varepsilon_j\rangle\langle r_j|$, and the corresponding passive state is $\tilde{\rho} = \sum_j r_j |\varepsilon_j\rangle\langle \varepsilon_j|$. The ergotropy \mathcal{E} can then be obtained explicitly as [1]

$$\mathcal{E} = \sum_k \varepsilon_k (\rho_{kk} - r_k), \quad (2)$$

where $\rho_{kk} = \sum_j r_j |\langle r_j | \varepsilon_k \rangle|^2$ is the k th diagonal element of ρ in the energy eigenbasis $\{|\varepsilon_k\rangle\}$ of H .

The ergotropy \mathcal{E} can be divided into two components, i.e., the incoherent and coherent components [11]. The incoherent component \mathcal{E}_i corresponds to the maximum work that can be extracted from the QB under coherence preserving operations $\mathcal{U}_c^{(i)}$, i.e.,

$$\mathcal{E}_i = \max_{V \in \mathcal{U}_c} \mathcal{W}(\rho, V), \quad (3)$$

where $V = \sum_k e^{-i\phi_k} |\varepsilon_k\rangle\langle \varepsilon_{\pi_k}| \equiv V_\pi$, with ϕ_k being an irrelevant phase factor and $\{\pi_k\}_{k=1,\dots,d}$ is a permutation of the elements of $\{1, \dots, d\}$. After optimizing over all possible $\{\pi_k\}_{k=1,\dots,d}$, one can obtain that the optimal $V_{\tilde{\pi}}$ ($\tilde{\pi}$ is the optimal permutation) yields $\sigma_\rho = V_{\tilde{\pi}} \rho V_{\tilde{\pi}}^\dagger = \sum_{kl} \rho_{\tilde{\pi}_k \tilde{\pi}_l} |\varepsilon_k\rangle\langle \varepsilon_l|$ [11], thus

$$\mathcal{E}_i = \sum_k \varepsilon_k (\rho_{kk} - \rho_{\tilde{\pi}_k \tilde{\pi}_k}), \quad (4)$$

where $\{\rho_{\tilde{\pi}_k \tilde{\pi}_k}\}_{k=1,\dots,d}$ is the rearrangement of the populations $\{\rho_{kk}\}_{k=1,\dots,d}$ in decreasing order. Equation (4) indicates that \mathcal{E}_i also equals to the ergotropy of the dephased state $\delta_\rho = \Delta[\rho] = \text{diag}\{\rho_{11}, \dots, \rho_{dd}\}$, i.e., $\mathcal{E}_i(\rho) = \mathcal{E}(\delta_\rho)$ [17], and the passive state associated with δ_ρ is $\tilde{\delta}_\rho = \text{diag}\{\rho_{\tilde{\pi}_1 \tilde{\pi}_1}, \dots, \rho_{\tilde{\pi}_d \tilde{\pi}_d}\}$.

Having defined the incoherent component \mathcal{E}_i , the coherent component of \mathcal{E} is naturally defined as $\mathcal{E}_c = \mathcal{E} - \mathcal{E}_i$, which, by combining Eqs. (2) and (4), can be obtained as

$$\mathcal{E}_c = \sum_k \varepsilon_k (\rho_{\tilde{\pi}_k \tilde{\pi}_k} - r_k), \quad (5)$$

and it quantifies the amount of work which cannot be extracted by using only incoherent operations.

III. THE CHARGER-BATTERY MODEL

The charger-battery model that we are going to discuss contains N qubits, all of which are placed inside a common zero-temperature bosonic reservoir in the vacuum initially. The total Hamiltonian (in units of \hbar), in the rotating wave approximation, can be written as

$$H = H_S + H_R + H_{\text{int}}, \quad (6)$$

where H_S and H_R , describe, respectively, the free Hamiltonians of the system and the reservoir, while H_{int} describes the interaction of the system with the reservoir. Their explicit forms are as follows:

$$\begin{aligned} H_S &= \omega_0 \sum_i \sigma_i^+ \sigma_i^-, \quad H_R = \sum_k \omega_k b_k^\dagger b_k, \\ H_{\text{int}} &= f(t) \sum_{i,k} g_k \sigma_i^+ b_k + \text{H.c.}, \end{aligned} \quad (7)$$

where ω_0 is the transition frequency between the ground state $|0\rangle$ and excited state $|1\rangle$ of each qubit, $\omega_0 \sigma_i^+ \sigma_i^-$ is actually the free Hamiltonian of the i th qubit, with σ_i^+ (σ_i^-) being the Pauli raising (lowering) operator. Moreover, b_k (b_k^\dagger) is the annihilation (creation) operator of the field mode k with frequency ω_k , and g_k is the coupling strength between each qubit and the field mode k of the reservoir. The function $f(t)$, which equals 1 for $t \in (0, \bar{t}]$ and 0 otherwise, is introduced for controlling the switchable coupling of the N qubits to the reservoir, where \bar{t} is the interaction time needed to charge the QB up to its (not necessary the first) dynamical maximum. When $t > \bar{t}$, the interaction between the qubits and the reservoir is switched off. Hereafter we call \bar{t} the charging time.

By treating the first n qubits as the charger and the other $N-n$ qubits the QB, the charging process can be implemented as follows. First, the ‘‘charger + battery’’ system is prepared in the state ρ_S , and its interaction with the reservoir is switched off at $t \leq 0$, that is, the initial state of the N -qubit system and the reservoir is $\rho = \rho_S \otimes |\bar{0}\rangle\langle \bar{0}|$, where $|\bar{0}\rangle$ is the vacuum state of the reservoir. When $t > 0$, the interaction between the N -qubit system and the reservoir is switched on, thereby there will be reservoir-mediated indirect interactions among the qubits, due to which the energy in the charger can be transferred to the QB in a wireless manner, and the common reservoir plays the role of a mediator between the two elements.

To elucidate the above wireless charging process, we need to solve the evolution equation of the N qubits. In this paper, we focus on the case in which the reservoir is the electromagnetic field inside a lossy cavity, which displays a Lorentzian broadening due to the nonperfect reflectivity of the cavity mirrors, and the spectral density is given by [68]

$$J(\omega) = \frac{\Omega^2}{\pi} \frac{\lambda}{(\omega - \omega_0)^2 + \lambda^2}, \quad (8)$$

where Ω is proportional to the vacuum Rabi frequency and λ denotes the frequency width of the spectrum. For such a model, if $N = 2$ (the single-charger case) and the ‘‘charger + battery’’ system is initialized in $v_{01}|10\rangle + v_{02}|01\rangle$ ($|v_{01}|^2 +$

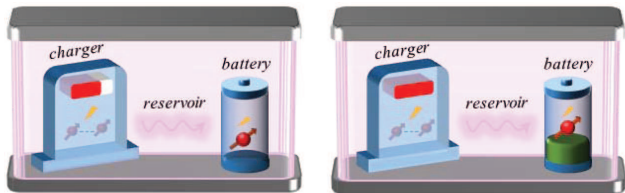


FIG. 1: Schematic representation of the wireless charging of the QB. (Left) Scenario I, where the charger is not in its excited state and the QB is empty initially. (Right) Scenario II, where the charger is in its excited state and the QB has residual ergotropy initially.

$|v_{02}|^2 = 1$), the dynamics of the system can be obtained analytically [68, 69], and the associated QB has been analyzed in Ref. [53, 54]. For the initial extended Werner-like states, analytical solutions of the two-qubit system can also be obtained in the Laplace transform space [70].

For a general initial state, it is hard to obtain the exact dynamics of the N -qubit system, even for $N = 2$. So we resort to the pseudomode approach, which describes the coherent interaction between the considered system and the pseudomodes [71–73]. Here, the pseudomodes are auxiliary variables defined from the spectrum of the reservoir. For $J(\omega)$ of Eq. (8), this approach results in the following pseudomode master equation in the interaction picture [71–75]:

$$\frac{\partial \varrho}{\partial t} = -i[V, \varrho] + \lambda(2a\varrho a^\dagger - a^\dagger a\varrho - \varrho a^\dagger a), \quad (9)$$

where a (a^\dagger) is the annihilation (creation) operator of the pseudomode, ϱ is the density operator of the extended system comprising the N -qubit system and the pseudomode, while the effective coupling between the N -qubit system and the pseudomode is described by the interaction Hamiltonian

$$V = \Omega \sum_i \sigma_i^+ a + \text{H.c.}, \quad (10)$$

by combining of which with Eq. (9), one can solve numerically the dynamics of ϱ without performing any further approximation. After having ϱ at hand, the density operator ρ for the N -qubit system can then be obtained via partial tracing of the pseudomode degrees of freedom, and likewise for the charger state ρ_{ch} and the battery state ρ_{ba} .

In alignment with Refs. [53, 68, 69], hereafter we use the dimensionless parameter $R = \sqrt{2}\Omega/\lambda$ to distinguish the strong coupling regime (good cavity, $R \gg 1$) from the weak one (bad cavity, $R \ll 1$), and due to the limited computing resource, we will focus on the cases of $N = 2, 3$, and 4, respectively.

IV. CHARGING THE QB WITH DIFFERENT CHARGERS

In this work, we consider the wireless charging of a QB for two different scenarios. For convenience of later presentation, we term them as scenarios I and II, respectively. As sketched in Fig. 1, scenario I refers to the case in which the charger is in the state $|\psi\rangle_{c_1 \dots c_n} = \otimes_{i=1}^n |\psi\rangle_{c_i}$ and the QB is in the ground

state $|0\rangle$ initially, while scenario II refers to the case in which the charger is in the fully excited state $|1\rangle^{\otimes n}$ and the QB is in the active state $|\varphi\rangle_{e_1}$ initially. The forms of $|\psi\rangle_{c_i}$ ($i = 1, \dots, n$) and $|\varphi\rangle_{e_1}$ are as follows:

$$\begin{aligned} |\psi\rangle_{c_i} &= \sqrt{c_i}|1\rangle + \sqrt{1-c_i}|0\rangle \quad (i = 1, \dots, n), \\ |\varphi\rangle_{e_1} &= \sqrt{e_1}|1\rangle + \sqrt{1-e_1}|0\rangle, \end{aligned} \quad (11)$$

where the parameters $c_i \in [0, 1]$ and $e_1 \in [0, 1]$.

For the scenario I, the n charging units are not in their excited states, that is, the charger energy is not maximal initially. So for the case of $n = 1$, even if the total energy in the charger is transferred to a QB, it cannot be fully charged. But this is a common situation encountered in practice, and it motivates us to consider the charging of an empty QB via n charging units having non-maximal energy, aimed at exploring whether it can complement the lack of energy in a single-charging unit. Here, by saying a QB is empty, we mean that no work can be extracted from it via any cyclic unitary transformation, that is, the battery state is passive. But this does not necessarily mean it is in the ground state. For the scenario II, there is residual ergotropy in the QB (i.e., $\mathcal{E} \neq 0$ initially), which is also a situation we may encounter, as we rarely wait until a battery runs out before charging. In particular, a traditional battery having residual energy may be charged faster than a fully discharged one. But whether this is indeed the case for a QB? This is our motivation for considering the scenario II.

Apart from the initial states in Eq. (11), we will also mention some other states (see below), e.g., the correlated charger states and mixed battery states.

A. The case of a single charging unit

For the case of a single charging unit (i.e., $n = 1$), when c_1 in Eq. (11) equals to 1, the charging of a QB has been investigated in Ref. [53, 54]. For the scenario I with different initial charger states $|\psi\rangle_{c_1}$, we show in the left column of Fig. 2 the dynamics of the ergotropy \mathcal{E} as well as its incoherent component \mathcal{E}_i and coherent component \mathcal{E}_c (in units of ω_0) in the good cavity limit $R = 20$. For this charger, its initial energy is $c_1\omega_0$, and the first dynamical maximum of \mathcal{E} is the maximal ergotropy charged on the QB, which, as shown by the different lines in Fig. 2(a), decreases with a decrease in c_1 . This is understandable as the charger energy also decreases with a decrease in c_1 . Moreover, our calculation shows that the energy is transferred to the QB from the very beginning, but as is shown in Fig. 2(a), the ergotropy \mathcal{E} remains zero for a finite time interval ($\lambda t \lesssim 0.1023$ when $R = 20$). This shows that the transferred energy cannot be converted into extractable work immediately in certain situations. As for the incoherent and coherent contributions to the ergotropy, by comparing the left three panels of Fig. 2, one can see that for the charger with a large c_1 , the incoherent contribution to ergotropy is dominant, whereas for that with a small c_1 , the coherent contribution to ergotropy turns to be dominant.

When considering the scenario II, we show in the right column of Fig. 2 the dynamics of \mathcal{E} , \mathcal{E}_i , and \mathcal{E}_c (in units of ω_0)

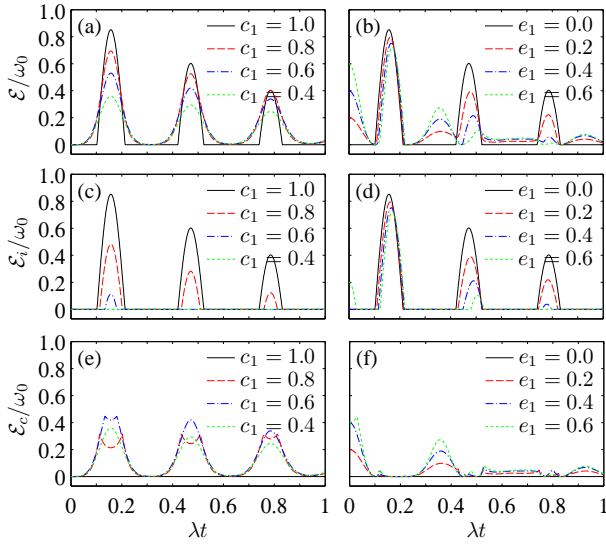


FIG. 2: Dynamics of \mathcal{E} , \mathcal{E}_i , and \mathcal{E}_c of the QB in the good cavity limit $R = 20$ for the case of a single charging unit. The left (right) three panels are plotted with the charger and QB being in the initial states $|\psi\rangle_{c_1}$ and $|0\rangle$ (I) and $|\varphi\rangle_{e_1}$, respectively.

in the good cavity limit $R = 20$. For this scenario, the initial state $|\varphi\rangle_{e_1}$ of the QB is active and the residual ergotropy in it is $e_1\omega_0$. From Fig. 2(b) one can see that \mathcal{E} first decays to zero (i.e., fully discharged) and then turns to be increased to its first dynamical maximum, and this can be recognized as the maximal ergotropy charged on the QB as the subsequent dynamical maxima become smaller and smaller. This phenomenon is in contrast to that of a traditional battery, as it indicates that when there is residual ergotropy in the QB, it will inevitably undergo a fully discharging process, after which it can then be continuously charged. Moreover, for a fixed R , the first dynamical maximum of \mathcal{E} may be smaller than its initial value $e_1\omega_0$ when e_1 is larger than a critical value (e.g., $e_1 \gtrsim 0.7129$ when $R = 20$), that is, the QB cannot be further charged in this case. Of course, the critical e_1 can be increased by increasing the coupling strength. By comparing the right three panels of Fig. 2, one can see that for this scenario, the incoherent contribution to ergotropy is always dominant, which is somewhat different from that of the scenario I.

In the above we have analyzed charging of a QB in the good cavity limit. Next, we see the case of the bad cavity limit. As is shown in Fig. 3(a), the ergotropy \mathcal{E} for the scenario I increases very slowly with the increase of λt , and the asymptotic value is much less than that in the good cavity limit. Physically, such an inefficiency has its roots in the weak coupling of the qubits to the reservoir, which induces a very weak indirect interaction between the the charger and the QB, so most of the energy in the charger is leaked into the reservoir. In particular, when $c_1 = 1$ (i.e., the charger is in its excited state), the QB cannot be charged at all. But this does not mean that there is no energy being transferred to the QB. In fact, in the infinite time limit one has $E_{ba}(\infty) = \text{tr}[\rho_{ba}(\infty)H_{ba}] = c_1\omega_0/4$ ($\forall c_1$) [it equals the injected energy as $E_{ba}(0) = 0$], where $\rho_{ba}(t)$ and H_{ba} are the density operator and free Hamiltonian of the QB,

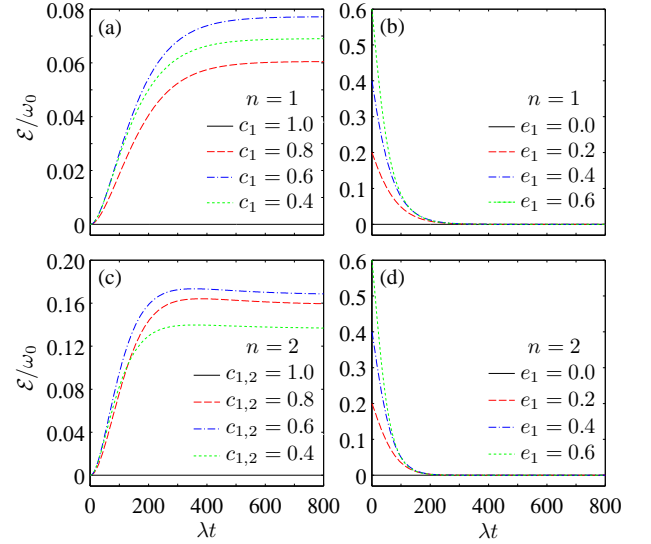


FIG. 3: Dynamics of \mathcal{E} of the QB in the bad cavity limit $R = 0.1$ for the case of n charging units. The left (right) two panels are plotted with the charger and QB being in the initial states $|\psi\rangle_{c_1\dots c_n}$ and $|0\rangle$ (I)²⁰ⁿ and $|\varphi\rangle_{e_1}$, respectively.

respectively. But when $c_1 = 1$, the energy E_{ba} cannot be extracted by means of any cyclic unitary transformation. This is because for this case the battery state $\rho_{ba} = \text{diag}\{e(t), 1 - e(t)\}$, where $e(t) < 0.25$ ($\forall t$). We have also calculated the incoherent and coherent components of \mathcal{E} (for the conciseness of this paper, we do not plot them here) and it is found that $\mathcal{E} \equiv \mathcal{E}_c$. As for the scenario II, although the initial battery state $|\varphi\rangle_{e_1}$ possesses nonzero ergotropy, from Fig. 3(b) one can note that \mathcal{E} always decays with the evolving time, thereby the QB cannot be charged in this case.

In the following, we examine charging rate of the QB characterized by the charging time \bar{t} . As is shown in the top two panels of Fig. 4, for the scenario I, $\lambda\bar{t}$ is independent of $c_1 \neq 0$ and it decreases monotonically with the increase of R . In the bad cavity limit, $\lambda\bar{t}$ will be infinitely large. On the contrary, it is very small in the good cavity limit (e.g., $\lambda\bar{t} \approx 0.0314$ for $R = 100$), that is, a fast charging is achieved. For the scenario II, $\lambda\bar{t}$ is weakly dependent on e_1 , and for a given e_1 it also decreases monotonically with the increasing R . This shows that the charging rate of a QB can be enhanced efficiently by increasing the coupling strength between the qubits (i.e., charger + QB) and the reservoir. Moreover, from Fig. 4(a) and (b) one can note that the charging times for the scenarios I and II are approximately the same, that is, the residual ergotropy in the QB does not help to improve the charging rate.

In the bottom two panels of Fig. 4, we show the R dependence of the ergotropy $\bar{\mathcal{E}}$ charged on the QB at $t = \bar{t}$. One can see that for both the scenarios I and II, $\bar{\mathcal{E}}$ increases monotonically with the increase of R . When $R \rightarrow \infty$, $\bar{\mathcal{E}}$ approaches its asymptotic value, which, for the scenario I, equals $c_1\omega_0$, and for the scenario II, equals ω_0 . This indicates that in theory, the energy in the charger is almost fully transferred to extractable work in the QB for such a limiting case. In fact, if the charger is in the excited state and QB is in the ground state, even for

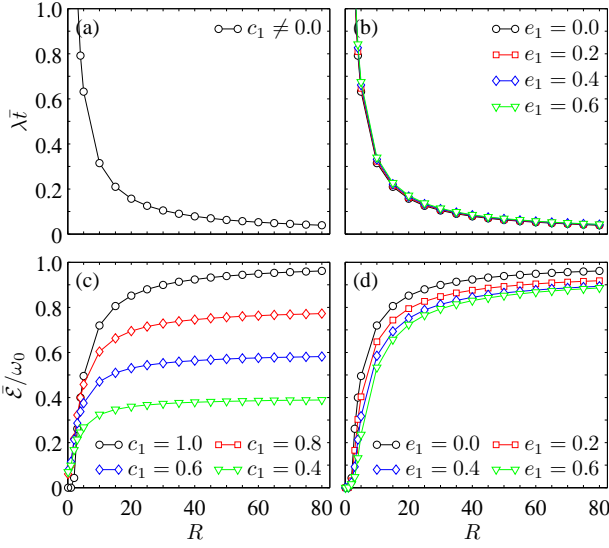


FIG. 4: The R dependence of the charging time $\lambda\bar{t}$ and ergotropy $\bar{\mathcal{E}}$ charged by a single charging unit at time \bar{t} . The left (right) two panels are plotted with the charger and QB being in the initial states $|\psi\rangle_{c_1}$ and $|0\rangle$ (I) and $|\varphi\rangle_{e_1}$, respectively. For small R , $\lambda\bar{t}$ is very large and the top two panels are cut to better visual its behavior in the large R region, and the first five points in (c) and (d) are plotted with $R = 0.1, 1, 2, 3,$ and 4 , respectively.

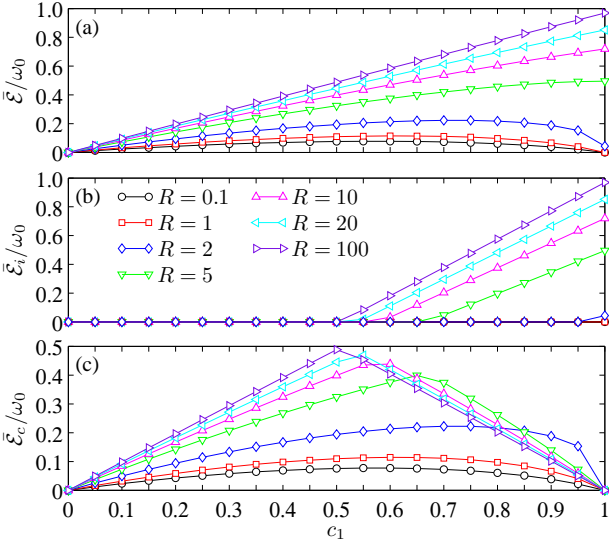


FIG. 5: The ergotropy $\bar{\mathcal{E}}$ and its incoherent component $\bar{\mathcal{E}}_i$ and coherent component $\bar{\mathcal{E}}_c$ (in units of ω_0) charged on the QB at time \bar{t} for the case of a single charging unit. The charger and QB are in the initial states $|\psi\rangle_{c_1}$ and $|0\rangle$, respectively. The circles and squares in (b) overlap with each other in the whole parameter region of c_1 .

the $R \simeq 10$ case which is experimentally accessible [76], the QB can be charged up to $\bar{\mathcal{E}} \simeq 0.72\omega_0$.

When R is finite, the ergotropy $\bar{\mathcal{E}}$ charged on a QB depends on c_1 and e_1 . To elucidate this in detail, we show in Fig. 5 the c_1 dependence of $\bar{\mathcal{E}}$ with the QB being in its ground state initially and in Fig. 6 the e_1 dependence of $\bar{\mathcal{E}}$ with the charger

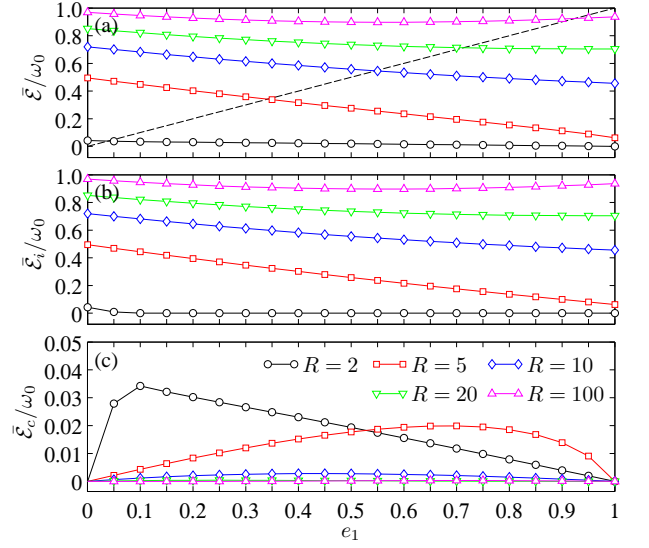


FIG. 6: The ergotropy $\bar{\mathcal{E}}$ and its incoherent component $\bar{\mathcal{E}}_i$ and coherent component $\bar{\mathcal{E}}_c$ (in units of ω_0) charged on the QB at time \bar{t} for the case of a single charging unit. The charger and QB are in the initial states $|1\rangle$ and $|\varphi\rangle_{e_1}$, respectively. In the region above the dashed line shown in (a), $\bar{\mathcal{E}}$ exceeds the initial ergotropy $e_1\omega_0$ in the QB.

being in the excited state initially. For the scenario I, when $c_1 = 0$, $\bar{\mathcal{E}} = 0$ by definition. When c_1 increases from 0 to 1, as depicted in Fig. 5(a), $\bar{\mathcal{E}}$ first increases to a small peak and then decreases to zero (e.g., $R = 0.1$ and 1) or to a small but finite value (e.g., $R = 2$) in the weak coupling regime. In the strong coupling regime, however, $\bar{\mathcal{E}}$ increases monotonically from 0 to its maximum; in particular, for large enough R (e.g., $R = 100$), it increases nearly linearly with the increase of c_1 . Moreover, by comparing the three panels in Fig. 5, one can also see that the coherent contribution to ergotropy is dominant when c_1 is relatively small, while this is not the case for large enough c_1 , and this phenomenon is consistent with that shown in Fig. 2. In particular, if the charger is in the excited state (i.e., $c_1 = 1$) initially, $\bar{\mathcal{E}} \equiv \bar{\mathcal{E}}_i$. This is because for this case, the battery state $\rho_{\text{ba}}(\bar{t})$ at time \bar{t} is diagonal, thereby there is no coherent contribution to the ergotropy [17].

For the scenario II, the QB is not fully discharged at the initial time, that is, there is residual ergotropy in it. For this case, when R is very small (i.e., the bad cavity limit), the QB cannot be charged, so we plot in Fig. 6 the case of $R \geq 2$, from which one can see that even for $R = 2$, the charged ergotropy $\bar{\mathcal{E}}$ is still very small, and it exceeds the initial ergotropy $e_1\omega_0$ of the QB only in a very narrow region of e_1 (i.e., $e_1 \lesssim 0.0382$). By increasing the coupling strength of the qubits and reservoir, $\bar{\mathcal{E}}$ can be noticeably enhanced. From Fig. 6(a) one can also see that the region of e_1 in which $\bar{\mathcal{E}}$ is larger than the initial ergotropy $e_1\omega_0$ expands with the increasing R . For example, for $R = 100$, the associated region can be obtained approximately as $e_1 \lesssim 0.9239$. As for the ratio of the incoherent and coherent components in $\bar{\mathcal{E}}$, from the bottom two panels of Fig. 6, one can see that apart from the small R case (e.g., $R = 2$), the incoherent contribution is always dominant, and this is different from that for the scenario I. We would also like to mention

that $\bar{\mathcal{E}}$ shown in Fig. 6(a) is not always a monotonic decreasing function of e_1 (or equivalently, the initial ergotropy in the QB), e.g., when $R = 100$ it takes a minimum at $e_1 \approx 0.5636$. Nonetheless, $\bar{\mathcal{E}}$ always takes its maximum at $e_1 = 0$, that is, the QB is in its ground state and empty initially. We have also examined the mixed battery state $\rho_{\text{ba}} = \text{diag}\{e_1, 1 - e_1\}$, which is empty for $e_1 \leq 0.5$, although its energy is $e_1\omega_0$. It is found that the charging performance is less efficient than that prepared in the ground state. In this sense, the optimal charging of a QB is achieved starting from its ground state, which is in agreement with the findings of Ref. [67].

Up to now, we have elucidated how the enlarged R helps to accelerate the charging rate and to pump more ergotropy (i.e., the maximal amount of extractable work) in the QB. Here, it is natural to ask another intriguing question: is the mean energy or ergotropy of the charger determines the ergotropy charged on a QB? As they always coexist for the free Hamiltonian H_{ch} [see Eq. (7)] and the initial state $|\psi\rangle_{c_1}$ [see Eq. (11)], we turn to consider a general one-qubit charger state ρ_{ch} and we first figure out the condition under which there is nonzero energy and zero ergotropy in it. After some algebra, one can obtain that this is achieved for $\rho_{\text{ch}} = \text{diag}\{c_1, 1 - c_1\}$ with $c_1 \leq 0.5$. In this case, the mean energy $c_1\omega_0$ in the charger equals to that for the initial state $|\psi\rangle_{c_1}$, and in the good cavity limit, most of the energy can be pumped in the QB. However, it is found that for any initial state (including the mixed one) of the QB, there is no ergotropy being charged on it. In this sense, it seems that it is the charger ergotropy instead of its energy determines the ergotropy charged on a QB.

To gain more insight into the wireless charging process of the QB, we can further consider dynamics of the mean energy E_{ch} and ergotropy \mathcal{E}_{ch} in the charger. Physically, as there is no direct interaction between the charger and the QB, the energy (ergotropy) in the charger will first being pumped in the reservoir and then charged into the QB via the reservoir-mediated indirect interaction. During such a dynamical process, partial of the energy (ergotropy) will inevitably be lost. Here, we focus on the case of not very small R and calculate the ergotropy in the charger with the same parameters as in Fig. 2 (for the conciseness of this paper, we do not show them here). For the scenario I, it is found that the ergotropy of the charger reaches its first dynamical minimum at $t = \bar{t}$, and such a minimum decreases with the increase of R , for example, for $R = 20$ it is of approximately 0. For the scenario II, however, the ergotropy \mathcal{E} in the QB does not always increase synchronously with the decrease of the ergotropy \mathcal{E}_{ch} in the charger. Specifically, the ergotropy for both the charger and the QB decays to zero after a short period of evolution time and then turns to be increased to the first dynamical maxima. However, the former decays to zero faster than the latter. This shows that there is a delayed effect for the ergotropy pumped in the reservoir to be charged into the QB.

B. The case of two charging units

In this subsection, we consider the case of two charging units, that is, the total number of qubits $N = 3$, where the first

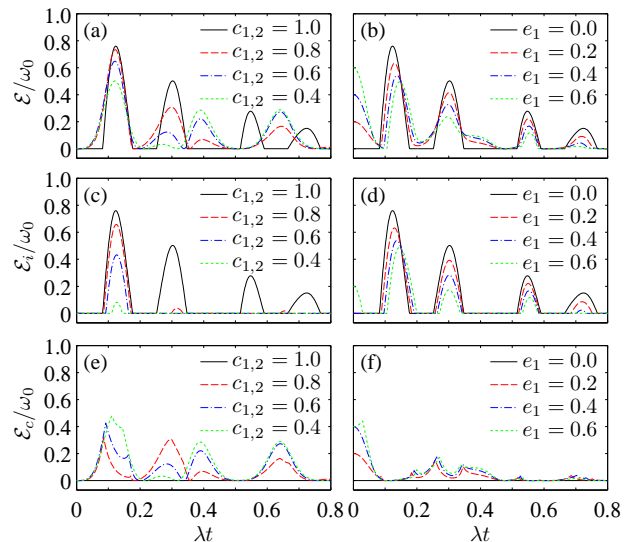


FIG. 7: Dynamics of \mathcal{E} , \mathcal{E}_i , and \mathcal{E}_c of the QB in the good cavity limit $R = 20$ for the case of two charging units. The left (right) three panels are plotted with the charger and QB being in the initial states $|\psi\rangle_{c_1 c_2}$ and $|0\rangle$ (|11) and $|\varphi\rangle_{e_1}$, respectively.

two qubits are treated as the charger (i.e., $n = 2$) and the third one as a QB. Intuitively, in this case the charger may produce a better result in ergotropy performance than that with a single charging unit as it possesses more energy and ergotropy. But is that really the case? This is our motivation for considering this problem. In particular, the presence of three qubits in the common reservoir makes the charging mechanism complex [6, 14, 17]. In the following, we investigate it in detail for the two scenarios of charging sketched in Fig. 1.

First, we show in Fig. 7 time evolution of \mathcal{E} , \mathcal{E}_i , and \mathcal{E}_c of the QB in the good cavity limit $R = 20$, where we have chosen $c_1 = c_2$ and the values of the system parameters are the same as those in Fig. 2. From this figure one can note that for both the scenarios I and II, \mathcal{E} shows a structurally similar behavior to that with a single charging unit. Moreover, although in this case the initial energy and ergotropy in the charger equal twice those for a single charging unit, the dynamical maximum $\bar{\mathcal{E}}$ is slightly decreased. This implies that the amounts of initial energy and ergotropy in the charger are not the only ingredients determining the ergotropy charged on a QB.

The incoherent and coherent components of ergotropy also show similar behaviors to those obtained for the case of a single charging unit shown in Fig. 2. Specifically, for the scenario I, the incoherent (coherent) contribution to ergotropy is dominant for the charger with a large (small) $c_{1,2}$, while for the scenario II, the incoherent contribution to ergotropy is always dominant. Looking at Fig. 7, one can also see that both \mathcal{E} and \mathcal{E}_i reach their first dynamical maxima at the same interaction time \bar{t} , but this is not the case for \mathcal{E}_c in general.

In the bad cavity limit $R = 0.1$, as exemplified in the bottom two panels of Fig. 3, the ergotropy \mathcal{E} also shows qualitatively the same behavior to that for the case of a single charging unit. But for the scenario I, apart from the special case of $c_{1,2} = 1$ for which \mathcal{E} always remains zero, the dynamical maximum of

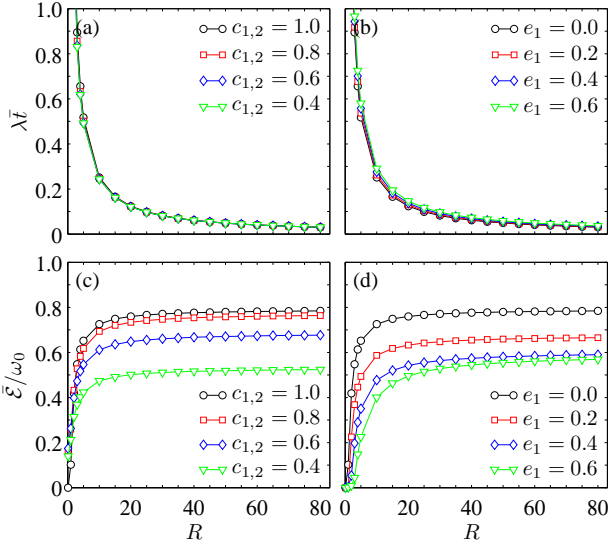


FIG. 8: The R dependence of the charging time $\lambda\bar{t}$ and ergotropy $\bar{\mathcal{E}}$ charged by two charging units at time \bar{t} . The left (right) two panels are plotted with the charger and QB being in the initial states $|\psi\rangle_{c_1c_2}$ and $|0\rangle$ (11) and $|\varphi\rangle_{e_1}$, respectively. For small R , $\lambda\bar{t}$ is very large and the top two panels are cut to better visual its behavior in the large R region, and the first five points in (c) and (d) are plotted with $R = 0.1, 1, 2, 3$ and 4 , respectively.

\mathcal{E} in this case is noticeably enhanced, and this phenomenon is in sharp contrast to that in the good cavity limit.

In Fig. 8, we show the R dependence of the charging time \bar{t} and the associated $\bar{\mathcal{E}}$ with different system parameters. First, one can see that its behavior is very similar to that for a single charging unit (cf. Fig. 4). Specifically, it is also insensitive to the variation of $c_{1,2}$ (scenario I) and e_1 (scenario II), especially in the strong coupling regime. By comparing Figs. 4 and 8, one can also find that $\lambda\bar{t}$ is slightly shortened in this case. Moreover, while $\bar{\mathcal{E}}$ also approaches an asymptotic value when $R \rightarrow \infty$, in contrast to the case of a single charging unit, such an asymptotic value is smaller than the initial energy $2c_1\omega_0$ (equals to the initial ergotropy) in the two charging units. In particular, for the scenario II with $e_1 \gtrsim 0.5911$ [see, e.g., the triangles in Fig. 8(d)], $\bar{\mathcal{E}}$ even cannot exceed its initial value $e_1\omega_0$, that is, the QB in this case cannot be charged anymore by the two charging units. This indicates that in the good cavity limit, the two charging units cannot outperform the single charging one if there is considerable amount of residual ergotropy in the QB initially. Of course, the case may be different for the finite R , and we will discuss this issue in detail after introducing the three charging units.

As we studied in the above only the initial product charger states, it is natural to ask whether the charging performance of a QB can be improved by using the initially quantum correlated charger states. To answer this question, we consider the following Bell-like charger states:

$$\begin{aligned} |\Psi^\pm\rangle &= \sqrt{c_1}|10\rangle \pm \sqrt{1-c_1}|01\rangle, \\ |\Phi^\pm\rangle &= \sqrt{c_1}|11\rangle \pm \sqrt{1-c_1}|00\rangle, \end{aligned} \quad (12)$$

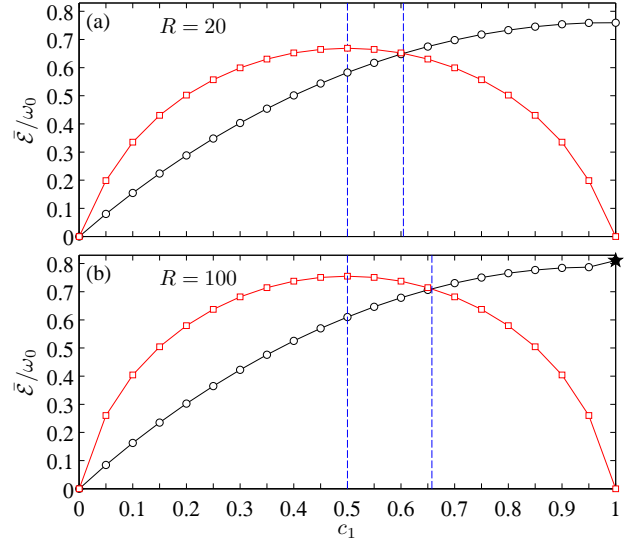


FIG. 9: Comparison of $\bar{\mathcal{E}}$ charged on a QB in the ground state initially, where the charger is in the initial state $|\psi\rangle_{c_1c_1}$ (circles) or $|\Psi^+\rangle$ (squares). The left dashed lines correspond to $c_1 = 0.5$ after which the charger energy $E_{\text{ch}}(|\Psi^+\rangle) < E_{\text{ch}}(|\psi\rangle_{c_1c_1})$, while the right dashed lines at $c_1 \approx 0.6045$ (a) and 0.6575 (b), respectively, show the critical points at which $\bar{\mathcal{E}}$ for $|\Psi^+\rangle$ equals to that for $|\psi\rangle_{c_1c_1}$. The star in (b) denotes the case for which $\bar{\mathcal{E}}$ corresponds to the second instead of the first dynamical maximum of \mathcal{E} .

and in Fig. 9 we give a plot of $\bar{\mathcal{E}}$ charged on a QB in its ground state by using the charger in the initial states $|\psi\rangle_{c_1c_1}$ and $|\Psi^+\rangle$, respectively. The initial charger energy is $E_{\text{ch}}(|\psi\rangle_{c_1c_1}) = 2c_1\omega_0$ and $E_{\text{ch}}(|\Psi^+\rangle) = \omega_0$ ($\forall c_1$), respectively, and so is the initial charger ergotropy. As shown in Fig. 9, in the parameter region between the two dashed vertical lines, $\bar{\mathcal{E}}$ for the initially correlated charger state is larger than that for the initially product charger state, though for the former case there is less energy in the charger. This indicates that, in certain situations, the correlated charger states are more efficient than that of the uncorrelated ones. But this is not a general conclusion; for example, a further calculation shows that the charger states $|\Psi^-\rangle$ and $|\Phi^\pm\rangle$ are less efficient than $|\psi\rangle_{c_1c_1}$. Moreover, as highlighted by the star in Fig. 9(b), the maximum ergotropy $\bar{\mathcal{E}}$ charged on a QB might correspond to the second instead of the first dynamical maximum of \mathcal{E} .

We have also examined time evolution of the ergotropy \mathcal{E}_{ch} in the two charging units, and for the conciseness of this paper, we also do not display them here. Note that \mathcal{E}_{ch} represents the ergotropy of the charger with respect to the total state ρ_{ch} of the two charging units, which is larger than the sum of the ergotropies with respect to the reduced states of the two charger qubits [1]. Similar to that for a single charging unit, the interaction time at which \mathcal{E}_{ch} reaches its first dynamical minimum is also not synchronously with the charging time \bar{t} at which the ergotropy charged on the QB reaches its dynamical maximum. Specifically, for the scenario I with not very small R , \mathcal{E}_{ch} reaches its first dynamical minimum after $t = \bar{t}$ if $c_{1,2}$ is very large (e.g., $c_{1,2} \gtrsim 0.9756$ when $R = 20$), while for the other $c_{1,2}$, it reaches its first dynamical minimum before $t = \bar{t}$.

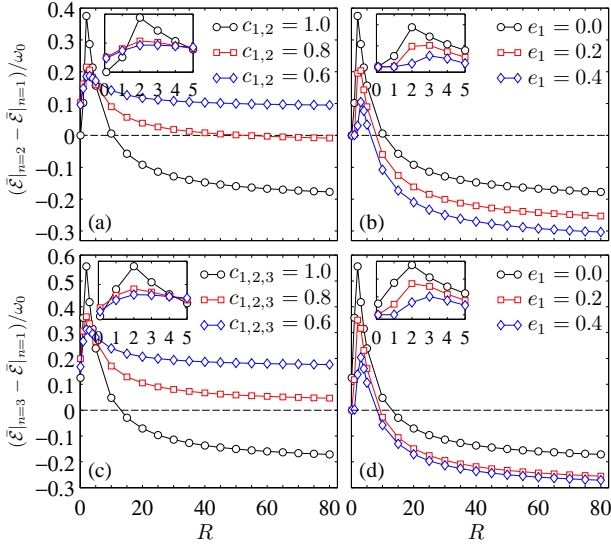


FIG. 10: Comparison of $\bar{\mathcal{E}}$ charged on the QB with different number n of charging units. The left (right) two panels are plotted with the chargers and QB being in the initial states $|\psi\rangle_{c_1\dots c_n}$ and $|0\rangle$ ($|1\rangle^{\otimes n}$ and $|\varphi\rangle_{e_1}$), respectively. The first five points in each panel are plotted with $R = 0.1, 1, 2, 3$ and 4 , respectively.

For the scenario II with not very small R , however, \mathcal{E}_{ch} reaches its first dynamical minimum after $t = \bar{t}$ for a very small e_1 (e.g., $e_1 \lesssim 0.0476$ when $R = 20$), and otherwise, it reaches its first dynamical minimum before $t = \bar{t}$. This indicates that the energy pumped in the reservoir previously can still be transferred to the QB in the time interval during which there is no additional energy to be injected into the reservoir.

C. The case of three charging units

When three qubits in the reservoir are treated as the charger ($n = 3$) and the fourth one as a QB, the behaviors of \mathcal{E} , \mathcal{E}_i , and \mathcal{E}_c are also structurally similar to those showed in Figs. 2 and 7, so we do not display them here. The charging time \bar{t} and the ergotropy $\bar{\mathcal{E}}$ charged on the QB at $t = \bar{t}$ also show qualitatively the similar R dependence to those showed in Figs. 4 and 8, so we also do not display them here. We only point out here that compared to those achieved with the two charging units, $\lambda\bar{t}$ for both the scenarios I and II can be further slightly shortened, while $\bar{\mathcal{E}}$ can also be enhanced to some extent.

Before ending to this section, we provide some further comparison about the charging of a QB by using different number of charging units. First, we present in Fig. 10 a comparison of the ergotropy, where we have denoted by $\bar{\mathcal{E}}_{n=1}$ the ergotropy charged on a QB with $n = 1$, and likewise for $\bar{\mathcal{E}}_{n=2}$ and $\bar{\mathcal{E}}_{n=3}$. For the scenario I, from Fig. 10(a) one can see that if $c_{1,2} = 1$, $\bar{\mathcal{E}}_{n=2} > \bar{\mathcal{E}}_{n=1}$ when $R \lesssim 10.34$, and this region expands with a decrease in $c_{1,2}$. This, together with Fig. 10(c), shows that if the charger energy is not maximal initially, one can enhance the ergotropy of the QB by using multiple charging units. As for the scenario II, from Fig. 10(b) one can observe that the region in which $\bar{\mathcal{E}}_{n=2} > \bar{\mathcal{E}}_{n=1}$ shrinks with the increase of e_1 .

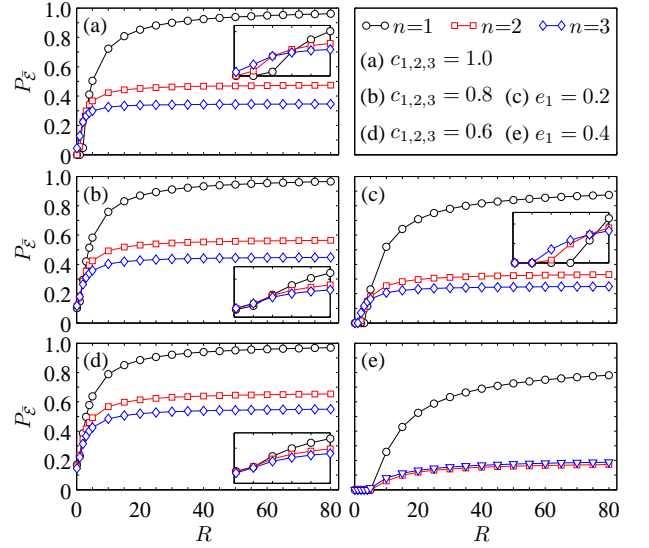


FIG. 11: Comparison of the charging efficiency $P_{\bar{\mathcal{E}}}$ for different number n of charging units. The left (right) panels are plotted with the charger and QB being in the initial states $|\psi\rangle_{c_1\dots c_n}$ and $|0\rangle$ ($|1\rangle^{\otimes n}$ and $|\varphi\rangle_{e_1}$), respectively. The parameters are given in the top right corner, and the insets show $P_{\bar{\mathcal{E}}}$ for $R = 0.1, 1, 2, 3, 4$, and 5 , respectively.

Although Fig. 10(d) shows that the ergotropy can be slightly enhanced for $n = 3$, the enhancement is limited. So in contrast to the scenario I, the performance of a QB can be enhanced by using multiple charging units only in the not very strong coupling regime. We have also compared the ergotropy charged on the initially mixed battery state $\rho_{\text{ba}} = \text{diag}\{e_1, 1 - e_1\}$ with different number of charging units, and a qualitatively similar phenomenon to that showed in Fig. 10 is observed.

One might also be concerned with the charging efficiency, that is, the proportion of output energy of the charger that can be converted into extractable work in the QB. To answer this question, we define

$$P_{\bar{\mathcal{E}}} = \frac{\Delta\bar{\mathcal{E}}}{\Delta E_{\text{ch}}} = \frac{\max\{0, \bar{\mathcal{E}}(\bar{t}) - \bar{\mathcal{E}}(0)\}}{\text{tr}\{[\rho_{\text{ch}}(0) - \rho_{\text{ch}}(\bar{t})]H_{\text{ch}}\}}, \quad (13)$$

where $\Delta\bar{\mathcal{E}}$ is the net ergotropy charged on the QB, ΔE_{ch} is the energy output from the charger, while $\rho_{\text{ch}}(\bar{t})$ denotes the state of the charger at time \bar{t} , and likewise for $\rho_{\text{ch}}(0)$. Based on this definition we performed numerical calculations and the result is shown in Fig. 11. Clearly, $P_{\bar{\mathcal{E}}}$ can be noticeably enhanced by increasing the coupling strength. In particular, for the scenario I with a single charging unit, if the QB is in its ground state initially (cf. the circles in the left column of Fig. 11), $P_{\bar{\mathcal{E}}}$ approaches 1 for large enough R . Moreover, for the case of not very weak coupling, $P_{\bar{\mathcal{E}}}$ decreases when n increases from 1 to 3, whereas this may not always be the case in the weak coupling regime. For the scenario II, as depicted in Fig. 11(c) and (e), if a single charging unit is considered, $P_{\bar{\mathcal{E}}}$ also approaches 1 when R approaches infinity, but in this case its increase with the increase of R is slower than that for the scenario I. When the two and three charging units are considered, although $P_{\bar{\mathcal{E}}}$ also increases with the increase of R , the asymptotic value at

$R \rightarrow \infty$ is obviously less than 1. This implies that a considerable amount of energy output from the charger is leaked into the reservoir in this situation.

Apart from $P_{\bar{\mathcal{E}}}$ in Eq. (13), we can also consider other definitions of the charging efficiency, e.g.,

$$\mathcal{P}_{\bar{\mathcal{E}}} = \frac{\Delta \bar{\mathcal{E}}}{\Delta E_{\text{ba}}} = \frac{\max\{0, \bar{\mathcal{E}}(\bar{t}) - \bar{\mathcal{E}}(0)\}}{\text{tr}\{[\rho_{\text{ba}}(\bar{t}) - \rho_{\text{ba}}(0)]H_{\text{ch}}\}}, \quad (14)$$

which is the proportion of input energy that can be extracted via the optimal cyclic unitary transformation. As its behavior is qualitatively similar to that in Fig. 11 and no new physics can be obtained, we do not plot them here.

V. SUMMARY AND DISCUSSION

In summary, we have studied the wireless charging of a QB via n ($n \geq 1$) charging units, where both the charger and the QB interact with a structured bosonic reservoir (which may be implemented, e.g., by an electromagnetic field inside a lossy cavity) and there is no direct coupling between them. Inspired by the fact that in realistic situation, the charger energy may be not maximal and one rarely wait until a battery runs out before charging, we considered two scenarios of wireless charging, that is, the scenario I in which the charger is in a superposition of the excited and ground states and the QB is empty (i.e., fully discharged) initially, and the scenario II in which the charger is in its excited state and the QB has residual ergotropy (i.e., partially discharged) initially. For both the scenarios, we considered the ergotropy, which quantifies the maximum amount of work a QB could supply during unitary cycles, as a figure of merit for comparing the charging performance. Our results showed that the charging time \bar{t} , defined as the interaction time at which the QB reaches its dynamical maximum, decreases with the increase of the coupling strength. The charging time \bar{t} also slightly shortens with an increase in the number of the charging units. The ergotropy $\bar{\mathcal{E}}$ charged on the QB at $t = \bar{t}$, on the other hand, increases with the increasing coupling strength. Specifically, if a single charging unit is used, then in the strong coupling regime, the ergotropy $\bar{\mathcal{E}}$ for the scenario I increases with the increasing amount of the initial energy in the charger, while that for the scenario II is not very sensitive to the residual ergotropy in the QB. In particular, the QB is almost fully charged when the coupling strength is strong enough. In the weak and moderate coupling regimes, however, the case will be different. The incoherent and coherent contributions to ergotropy are also different in different coupling regimes. Moreover, compared to the case of a single charging unit, the ergotropy $\bar{\mathcal{E}}$ charged by two and three charging units is decreased in the strong coupling regime, whereas in the weak and moderate coupling regimes, it can be enhanced to some extent; in particular, such an enhancement is pronounced for the scenario I in which the charger energy is not maximal, and this implies that in this situation the multiple charging units could compensate to some extent the lack of energy in a single charging unit. Finally, we have also considered the charging efficiency which quantifies the proportion of output energy that can be

converted into extractable work in the QB. It was found that it also increases with the increase of the coupling strength. If a single charging unit is considered, this efficiency approaches 1 when $R \rightarrow \infty$, while for that of the two and three charging units, it is significantly decreased.

While we considered in this paper the charging of a single-cell QB via n charging units, one may also be concerned with the general case in which a m -cell QB is charged via n charging units. Although it is hard to obtain a general result for this case due to the limited computing resource, we performed numerical calculations with $n + m \leq 4$ and the results showed that for $m = 2$ and 3, the dynamical behavior of \mathcal{E} is structurally similar to that for a single-cell QB, and the maximum ergotropy $\bar{\mathcal{E}}$ charged on a QB can also be noticeably enhanced by increasing the coupling strength, but now it cannot be fully charged, even if R approaches infinity. Moreover, similar to that showed in Fig. 9(b), if the charger and QB are in the initial states $|11\rangle$ and $|00\rangle$ (i.e., $n = 2$ and $m = 2$), respectively, the maximum ergotropy $\bar{\mathcal{E}}$ also corresponds to the second instead of the first dynamical maximum of \mathcal{E} when $R \gtrsim 34$. It is also interesting that the ergotropy $\bar{\mathcal{E}}$ charged on a two-cell QB is much larger than that charged on a single-cell QB when using the same two charging units. This suggests that, in general, the charging process of a QB is extremely complex. It depends on the initial energy and ergotropy in the charger, the residual energy and ergotropy in the QB, as well as the coupling manner and coupling strength between them. To find more intrinsic relations underlying these elements and to identify essential ingredients boosting the charging performance of a QB is an intriguing direction. This will not only help us to have a better understanding on the charging mechanism, but can also help us to develop the high-efficiency QB.

Moreover, it is natural for future work to consider the case that the charger and the QB are coupled to a common reservoir with different strengths, just as the two-qubit case studied in Ref. [53], or further consider the case that there is frequency detuning between the qubits and the cavity field, for which the off-resonant effect on generation of two-qubit entanglement has been studied [68, 69]. In addition, one can also generalize the results in this work to the structured reservoir, which acts as a mediator between the charger and QB, with other kinds of spectra (e.g., the sub-Ohmic, Ohmic, and super-Ohmic spectral densities [77]). Of course, in these cases we first need to solve the dynamical equation of the system for a general instead of a special multi-qubit initial state, which may be a very intricate and challenging task.

ACKNOWLEDGMENTS

This work was supported by the National Natural Science Foundation of China (Grant No. 12275212, No. T2121001, No. 92265207, and No. 92365301), Shaanxi Fundamental Science Research Project for Mathematics and Physics (Grant No. 22JSY008), the Youth Innovation Team of Shaanxi Universities, and Technology Innovation Guidance Special Fund of Shaanxi Province (Grant No. 2024QY-SZX-17).

-
- [1] A. E. Allahverdyan, R. Balian, and Th. M. Nieuwenhuizen, *Europhys. Lett.* **67**, 565 (2004).
- [2] W. Pusz and S. L. Woronowicz, *Commun. Math. Phys.* **58**, 273 (1977).
- [3] A. Lenard, *J. Stat. Phys.* **19**, 575 (1978).
- [4] M. Alimuddin, T. Guha, and P. Parashar, *Phys. Rev. E* **102**, 022106 (2020).
- [5] R. Alicki and M. Fannes, *Phys. Rev. E* **87**, 042123 (2013).
- [6] K. V. Hovhannisyanyan, M. Perarnau-Llobet, M. Huber, and A. Acín, *Phys. Rev. Lett.* **111**, 240401 (2013).
- [7] M. Perarnau-Llobet, K. V. Hovhannisyanyan, M. Huber, P. Skrzypczyk, N. Brunner, and A. Acín, *Phys. Rev. X* **5**, 041011 (2015).
- [8] A. Mukherjee, A. Roy, S. S. Bhattacharya, and M. Banik, *Phys. Rev. E* **93**, 052140 (2016).
- [9] G. M. Andolina, M. Keck, A. Mari, M. Campisi, V. Giovannetti, and M. Polini, *Phys. Rev. Lett.* **122**, 047702 (2019).
- [10] L. P. García-Pintos, A. Hamma, and A. del Campo, *Phys. Rev. Lett.* **125**, 040601 (2020).
- [11] G. Francica, F. C. Binder, G. Guarnieri, M. T. Mitchison, J. Goold, and F. Plastina, *Phys. Rev. Lett.* **125**, 180603 (2020).
- [12] B. Çakmak, *Phys. Rev. E* **102**, 042111 (2020).
- [13] F. H. Kamin, F. T. Tabesh, and S. Salimi, *Phys. Rev. E* **102**, 052109 (2020).
- [14] J. X. Liu, H. L. Shi, Y. H. Shi, X. H. Wang, and W. L. Yang, *Phys. Rev. B* **104**, 245418 (2021).
- [15] G. Francica, *Phys. Rev. E* **105**, L052101 (2022).
- [16] M. B. Arjmandi, A. Shokri, E. Faizi, and H. Mohammadi, *Phys. Rev. A* **106**, 062609 (2022).
- [17] H. L. Shi, S. Ding, Q. K. Wan, X. H. Wang, and W. L. Yang, *Phys. Rev. Lett.* **129**, 130602 (2022).
- [18] X. Yang, Y. H. Yang, M. Alimuddin, R. Salvia, S. M. Fei, L. M. Zhao, S. Nimmrichter, and M. X. Luo, *Phys. Rev. Lett.* **131**, 030402 (2023).
- [19] H. Y. Yang, H. L. Shi, Q. K. Wan, K. Zhang, X. H. Wang, and W. L. Yang, *Phys. Rev. A* **109**, 012204 (2024).
- [20] T. P. Le, J. Levinsen, K. Modi, M. M. Parish, and F. A. Pollock, *Phys. Rev. A* **97**, 022106 (2018).
- [21] D. Rossini, G. M. Andolina, and M. Polini, *Phys. Rev. B* **100**, 115142 (2019).
- [22] S. Ghosh, T. Chanda, and A. Sen(De), *Phys. Rev. A* **101**, 032115 (2020).
- [23] F. Q. Dou, H. Zhou, and J. A. Sun, *Phys. Rev. A* **106**, 032212 (2022).
- [24] W. Lu, J. Chen, L. M. Kuang, and X. Wang, *Phys. Rev. A* **104**, 043706 (2021).
- [25] D. Farina, G. M. Andolina, A. Mari, M. Polini, and V. Giovannetti, *Phys. Rev. B* **99**, 035421 (2019).
- [26] G. M. Andolina, D. Farina, A. Mari, V. Pellegrini, V. Giovannetti, and M. Polini, *Phys. Rev. B* **98**, 205423 (2018).
- [27] Y. V. de Almeida, T. F. F. Santos, and M. F. Santos, *Phys. Rev. A* **108**, 052218 (2023).
- [28] L. Fusco, M. Paternostro, and G. D. Chiara, *Phys. Rev. E* **94**, 052122 (2016).
- [29] D. Ferraro, M. Campisi, G. M. Andolina, V. Pellegrini, and M. Polini, *Phys. Rev. Lett.* **120**, 117702 (2018).
- [30] Y. Y. Zhang, T. R. Yang, L. Fu, and X. Wang, *Phys. Rev. E* **99**, 052106 (2019).
- [31] F. Q. Dou, Y. Q. Lu, Y. J. Wang, and J. A. Sun, *Phys. Rev. B* **105**, 115405 (2022).
- [32] A. C. Santos, B. Çakmak, S. Campbell, and N. T. Zinner, *Phys. Rev. E* **100**, 032107 (2019).
- [33] F. Campaioli, F. A. Pollock, F. C. Binder, L. Céleri, J. Goold, S. Vinjanampathy, and K. Modi, *Phys. Rev. Lett.* **118**, 150601 (2017).
- [34] F. Pirmoradian and K. Mølmer, *Phys. Rev. A* **100**, 043833 (2019).
- [35] K. V. Hovhannisyanyan, F. Barra, and A. Imparato, *Phys. Rev. Research* **2**, 033413 (2020).
- [36] A. C. Santos, A. Saguia, and M. S. Sarandy, *Phys. Rev. E* **101**, 062114 (2020).
- [37] L. Peng, W. B. He, S. Chesi, H. Q. Lin, and X. W. Guan, *Phys. Rev. A* **103**, 052220 (2021).
- [38] S. Ghosh and A. Sen(De), *Phys. Rev. A* **105**, 022628 (2022).
- [39] A. Crescente, M. Carrega, M. Sassetti, and D. Ferraro, *Phys. Rev. B* **102**, 245407 (2020).
- [40] M. B. Arjmandi, H. Mohammadi, A. Saguia, and M. S. Sarandy, *Phys. Rev. E* **108**, 064106 (2023).
- [41] P. Chen, T. S. Yin, Z. Q. Jiang, and G. R. Jin, *Phys. Rev. E* **106**, 054119 (2022).
- [42] F. C. Binder, S. Vinjanampathy, K. Modi, and J. Goold, *New J. Phys.* **17**, 075015 (2015).
- [43] G. M. Andolina, M. Keck, A. Mari, V. Giovannetti, and M. Polini, *Phys. Rev. B* **99**, 205437 (2019).
- [44] D. Rossini, G. M. Andolina, D. Rosa, M. Carrega, and M. Polini, *Phys. Rev. Lett.* **125**, 236402 (2020).
- [45] A. C. Santos, *Phys. Rev. E* **103**, 042118 (2021).
- [46] S. Seah, M. Perarnau-Llobet, G. Haack, N. Brunner, and S. Nimmrichter, *Phys. Rev. Lett.* **127**, 100601 (2021).
- [47] J. Y. Gyhm, D. Šafránek, and D. Rosa, *Phys. Rev. Lett.* **128**, 140501 (2022).
- [48] T. F. F. Santos, Y. V. de Almeida, and M. F. Santos, *Phys. Rev. A* **107**, 032203 (2023).
- [49] R. Salvia, M. Perarnau-Llobet, G. Haack, N. Brunner, and S. Nimmrichter, *Phys. Rev. Research* **5**, 013155 (2023).
- [50] S. Julià-Farré, T. Salamon, A. Riera, M. N. Bera, and M. Lewenstein, *Phys. Rev. Research* **2**, 023113 (2020).
- [51] S. Zakavati, F. T. Tabesh, and S. Salimi, *Phys. Rev. E* **104**, 054117 (2021).
- [52] F. Barra, *Phys. Rev. Lett.* **122**, 210601 (2019).
- [53] F. T. Tabesh, F. H. Kamin, and S. Salimi, *Phys. Rev. A* **102**, 052223 (2020).
- [54] F. H. Kamin, F. T. Tabesh, S. Salimi, F. Kheirandish, and A. C. Santos, *New J. Phys.* **22**, 083007 (2020).
- [55] M. Carrega, A. Crescente, D. Ferraro, and M. Sassetti, *New J. Phys.* **22**, 083085 (2020).
- [56] J. Q. Quach and W. J. Munro, *Phys. Rev. Appl.* **14**, 024092 (2020).
- [57] W. Chang, T. R. Yang, H. Dong, L. Fu, X. Wang, and Y. Y. Zhang, *New J. Phys.* **23**, 103026 (2021).
- [58] S. Ghosh, T. Chanda, S. Mal, and A. Sen(De), *Phys. Rev. A* **104**, 032207 (2021).
- [59] M. L. Song, L. J. Li, X. K. Song, L. Ye, and D. Wang, *Phys. Rev. E* **106**, 054107 (2022).
- [60] M. B. Arjmandi, H. Mohammadi, and A. C. Santos, *Phys. Rev. E* **105**, 054115 (2022).
- [61] K. Xu, H. G. Li, Z. G. Li, H. J. Zhu, G. F. Zhang, and W. M. Liu, *Phys. Rev. A* **106**, 012425 (2022).
- [62] F. Mayo and A. J. Roncaglia, *Phys. Rev. A* **105**, 062203 (2022).
- [63] J. Carrasco, J. R. Maze, C. Hermann-Avigliano, and F. Barra, *Phys. Rev. E* **105**, 064119 (2022).
- [64] F. Centrone, L. Mancino, and M. Paternostro, *Phys. Rev. A* **108**,

- 052213 (2023).
- [65] L. Wang, S. Q. Liu, F. L. Wu, H. Fan, and S. Y. Liu, *Phys. Rev. A* **108**, 062402 (2023).
- [66] W. L. Song, H. B. Liu, B. Zhou, W. L. Yang, and J. H. An, *Phys. Rev. Lett.* **132**, 090401 (2024).
- [67] A. Crescente, M. Carrega, M. Sassetti, and D. Ferraro, *New J. Phys.* **22**, 063057 (2020).
- [68] S. Maniscalco, F. Francica, R. L. Zaffino, N. L. Gullo, and F. Plastina, *Phys. Rev. Lett.* **100**, 090503 (2008).
- [69] F. Francica, S. Maniscalco, J. Piilo, F. Plastina, and K.-A. Suominen, *Phys. Rev. A* **79**, 032310 (2009).
- [70] L. Mazzola, S. Maniscalco, J. Piilo, and K.-A. Suominen, *J. Phys. B* **43**, 085505 (2010).
- [71] B. M. Garraway, *Phys. Rev. A* **55**, 2290 (1997).
- [72] B. J. Dalton, S. M. Barnett, and B. M. Garraway, *Phys. Rev. A* **64**, 053813 (2001).
- [73] B. J. Dalton and B. M. Garraway, *Phys. Rev. A* **68**, 033809 (2003).
- [74] L. Mazzola, S. Maniscalco, J. Piilo, K.-A. Suominen, and B. M. Garraway, *Phys. Rev. A* **79**, 042302 (2009).
- [75] D. Z. Rossato, T. Werlang, L. K. Castelano, C. J. Villas-Boas, and F. F. Fanchini, *Phys. Rev. A* **84**, 042113 (2011).
- [76] S. Kuhr, S. Gleyzes, C. Guerlin, J. Bernu, U. B. Hoff, S. Deléglise, S. Osnaghi, M. Brune, J.-M. Raimond, S. Haroche, E. Jacques, P. Bosland, and B. Visentin, *Appl. Phys. Lett.* **90**, 164101 (2007).
- [77] A. J. Leggett, S. Chakravarty, A. T. Dorsey, M. P. A. Fisher, A. Garg, and W. Zwerger, *Rev. Mod. Phys.* **59**, 1 (1987).